

Supplementary Material for “**Density functional theory based
molecular dynamics study of solution composition effects on
the solvation shell of metal ions**”

*Xiangwen Wang,^a Dimitrios Toroz,^a Seonmyeong Kim,^{b,c} Simon Clegg,^d Gun-Sik
Park,^{b,c} and Devis Di Tommaso,^{*, a}*

^a Thomas Young Centre, Materials Research Institute and Department of Chemistry,
Queen Mary University of London, Mile End Road, London, E1 4NS, United Kingdom

^b Center for THz-driven Biomedical Systems, Seoul National University, Department of
Physics and Astronomy, Seoul National University, Seoul, 08826, Republic of Korea

^c Seoul National University, Advanced Institutes of Convergence Technology, Suwon-Si,
Gyeonggi-do 16229, Republic of Korea

^d School of Environmental Sciences, University of East Anglia, Norwich, NR4 7TJ,
United Kingdom

Corresponding Author

* E-mail: d.ditommaso@qmul.ac.uk

Table of Contents

Simulation details	3
Cation hydration structure	4
Ion pairing in solution.....	6
Dynamics of ionic hydration shell.....	8
Water exchange around metal ions.....	8
Free energy profiles of metal ion dehydration.....	9
Velocity autocorrelation function of the metal ions	11
Hydrogen bond statistics.....	13
Calculation of time correlation functions	14
Protocol.....	14
Time average of time correlation functions over several time origin.....	15
References.....	18

Simulation details

TABLE S1. Details of the electrolyte solutions: concentration (b) in mol.kg⁻¹, number of units and H₂O molecules, cell length after classical MD (NPT) simulation, and total time duration (t_{sim}) of each AIMD simulation.

System		b	n_{units}	n_{water}	Cell length (Å)	t_{sim}
Li ⁺	1	0.9	1	63	12.5	50
LiCl	2	1.9	2	60	12.6	50
Na ⁺	3	0.9	1	63	12.5	50
NaCl	4	0.9	1	62	12.3	50
	5	1.9	2	60	12.3	50
	6	3.8	4	58	12.2	50
K ⁺	7	0.9	1	63	12.5	50
KCl	8	0.9	1	62	12.4	50
	9	1.9	2	60	12.4	50
	10	3.8	4	58	12.6	50
Cs ⁺	11	0.9	1	63	12.5	50
CsCl	12	1.9	2	60	12.7	50
Mg ²⁺	13	0.9	1	63	12.3	40
MgCl ₂	14	1.9	2	58	12.5	50
MgSO ₄	15	1.9	2	60	12.9	50
Ca ²⁺	16	0.9	1	63	12.4	500
CaCl ₂	17	1.9	2	58	12.5	50
CaSO ₄	18	1.9	2	60	12.7	50
Bulk water	19	0.0	–	64	12.4	50
Cl ⁻	20	0.9	1	63	12.5	40

Cation hydration structure

TABLE S2. Structural properties of the cation–water radial distribution functions obtained from the AIMD simulations of the hydrated ions (isolated ion, no counterion) in 63 water molecules conducted in this study. The positions, r_{\max} , and amplitudes, $g(r_{\max})$, of first peak and the average coordination number (CN) of the cation hydration shell are compared with other AIMD studies and available experimental data. Distances in Å.

System	Reference	Method ^{a)}	Functional	Pseudopot. ^{b)}	Basis set ^{c)}	r_{\max}	$g(r_{\max})$	CN
Li ⁺	This study	BOMD	PBE-D3	GTH	DZVP/PW (1000 Ry)	1.98	9.4	4.0
	Lyubartsev ¹	CPMD	BLYP	USPP	PW (25 Ry)	1.96	9.5	
Na ⁺	This study	BOMD	PBE-D3	GTH	DZVP/PW (1000 Ry)	2.41	5.0	5.1
		BOMD	revPBE-D3	GTH	DZVP/PW (1000 Ry)	2.53	4.6	5.6
	Duignan et al. ²	BOMD	revPBE-D3	GTH	DZVP/PW (400 Ry)	2.51	4.1	
		BOMD	SCAN	GTH	DZVP/PW (1200 Ry)	2.36	5.9	
	Galib et al. ³	BOMD	revPBE	GTH	TZV2P/PW (400 Ry)	2.45	5.8	5.7
		BOMD	revPBE-D3	GTH	TZV2P/PW (400 Ry)	2.53	4.8	6.0
		BOMD	revPBE	GTH	DZVP/PW (400 Ry)	2.46	5.7	5.7
		BOMD	revPBE-D3	GTH	DZVP/PW (400 Ry)	2.56	4.0	6.1
		BOMD	BLYP	GTH	TZV2P/PW (400 Ry)	2.40	5.9	4.9
		BOMD	BLYP-D2	GTH	TZV2P/PW (400 Ry)	2.46	6.4	5.7
NaCl (6 m)	Galib et al. ³	EXAFS			2.37		5.4	
		XRD			2.38		5.5	
NaCl (2.5 m)	Galib et al. ³	XRD			2.38		5.9	
K ⁺	This study	BOMD	PBE-D3	GTH	DZVP/PW (1000 Ry)	2.80	3.4	6.2
		BOMD	revPBE-D3	GTH	DZVP/PW (400 Ry)	2.98	3.1	
	Duignan et al. ²	BOMD	SCAN	GTH	DZVP/PW (1200 Ry)	2.78	3.8	
		Glezakou et al. ⁴	EXAFS			2.76		6.1
Cs ⁺	This study	BOMD	PBE-D3	GTH	DZVP/PW (1000 Ry)	3.17	2.7	5.9
		BOMD	PBE-D3	PAW	PW (30 Ry)	3.15	3.3	
Mg ²⁺	This study	BOMD	PBE-D3	GTH	DZVP/PW (1000 Ry)	2.11	13.5	6.0
		CPMD	PBE	USPP	PW (30 Ry)	2.08	12.3	6.0
	Di Tommaso ⁶	Callahan et al. ⁷	XRD			2.0-2.12		6.0
Ca ²⁺	This study	BOMD	PBE	GTH	DZVP/PW (1000 Ry)	2.40	10.8	6.0
		BOMD	PBE-D3	GTH	DZVP/PW (1000 Ry)	2.40	10.2	6.0
		BOMD	BLYP	GTH	DZVP/PW (1000 Ry)	2.40	9.6	6.3
		BOMD	BLYP-D3	GTH	DZVP/PW (1000 Ry)	2.42	9.9	6.8
		BOMD	revPBE	GTH	DZVP/PW (1000 Ry)	2.43	9.4	6.6
		BOMD	revPBE-D3	GTH	DZVP/PW (1000 Ry)	2.39	10.8	6.1
	Di Tommaso et al. ⁶	CPMD	PBE-D3	GTH	DZVP/PW (1000 Ry)	2.36	8.5	6.4
	Bako et al. ⁸	CPMD	BLYP	NCPP	PW (70 Ry)	2.45	10.5	6
	CaCl ₂ (6 m)	Fulton et al. ⁹				2.43		7.2

^{a)} BOMD = Born-Oppenheimer molecular dynamics, CPMD = Car-Parrinello Molecular Dynamics. ^{b)} GTH = Goedecker-Teter-Hutter; USPP = Ultra-Soft Pseudopotential; PAW = projector augmented wave; NCPP = Norm-Conserving Pseudopotential. ^{c)} DZVP = double-zeta valence polarized; TZV2P = triple-zeta valence doubly polarized; PW = plane wave.

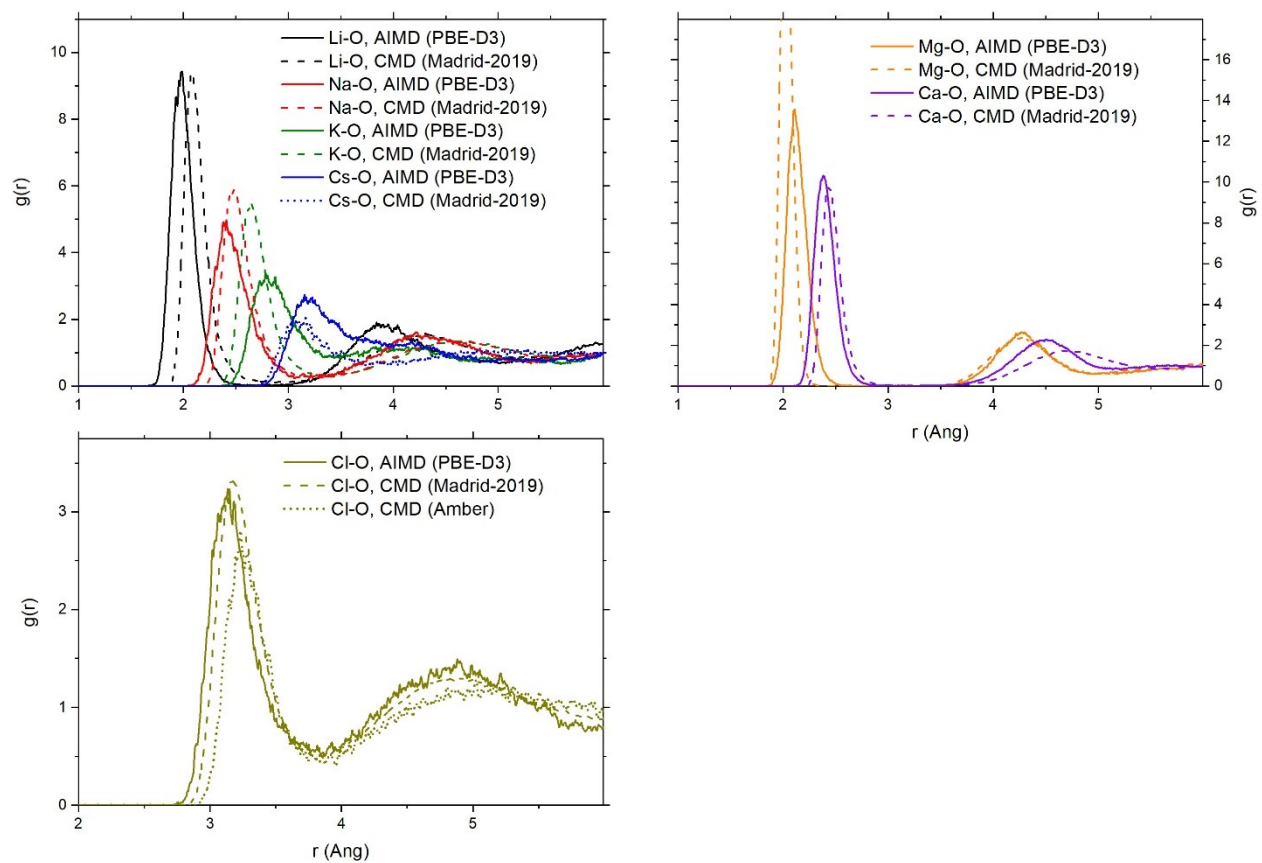


Figure S1. Ion-water radial distribution functions obtained from ab initio MD (PBE-D3) and classical MD (Madrid-2019 and Amber) methods.

Ion pairing in solution

TABLE S3 The speciation of M^{n+} (Li^+ , Na^+ , K^+ , Cs^+ , Mg^{2+} and Ca^{2+}) with the counterions (X) chloride (Cl^-) or sulphate (SO_4^{2-}) as a function of concentration determined in terms of the following ion pairing criteria: contact ion pair (CIP) when M^{n+} and X^{n-} are in direct physical contact; solvent-shared ion pairs (SSHIP) when M^{n+} and X^{n-} are separated by one water molecule; solvent-separated ion pairs (SSIP) when M^{n+} and X^{n-} are separated by at least two water molecules. These assignments were from to the analysis of the M–X radial distribution functions (RDFs): CIP if $r_{M-X} \leq r_{M-X}^{min1}$; SSHIP if $r_{M-X}^{min1} < r_{M-X} \leq r_{M-X}^{min2}$; SSIP if $r_{M-X} > r_{M-X}^{min2}$ where r_{M-X}^{min1} and r_{M-X}^{min2} are the positions of the first and second minima, respectively, of the M–X, radial distribution functions. Results obtained from the analysis of AIMD (PBE-D3) simulations. Concentration (b) in mol.kg⁻¹.

System		b	CIP (%)	SSHIP (%)	SSIP (%)
LiCl	2	1.9	85.6	14.4	0.0
NaCl	4	0.9	0.0	0.0	100
	5	1.9	0.0	68.9	31.1
	6	3.8	43.9	55.9	0.2
	8	0.9	36.1	59.1	4.8
KCl	9	1.9	3.3	51.4	45.3
	10	3.8	65.6	34.1	0.2
	12	1.9	72.8	27.2	0.0
CsCl	12	1.9	72.8	27.2	0.0
MgCl ₂	14	1.9	0.0	55.5	44.5
MgSO ₄	15	1.9	100.0	0.0	0.0
CaCl ₂	17	1.9	0.7	97.1	2.2
CaSO ₄	18	1.9	0.0	99.6	0.4

TABLE S4. Number of accounted exchanges of water ($N_{ex,H2O}$) and chlorine ($N_{ex,Cl}$) in the first coordination shells of the metal ions Na^+ , K^+ , and Cs^+ , with a duration of more than $t > 0.5$ ps, obtained from the analysis of 50 ps of AIMD (PBE-D3) simulations of 1.9 mol kg⁻¹ aqueous electrolyte solution. Values normalized to the number of metal ions in solution. Also reported are the values of $f_{ex} = N_{ex,H2O} / N_{ex,Cl}$.

System	$N_{ex,H2O}$	$N_{ex,Cl}$	f_{ex}
NaCl	195.5	46.5	4.2
KCl	693.5	26.5	26.2
CsCl	983.0	36.5	26.9

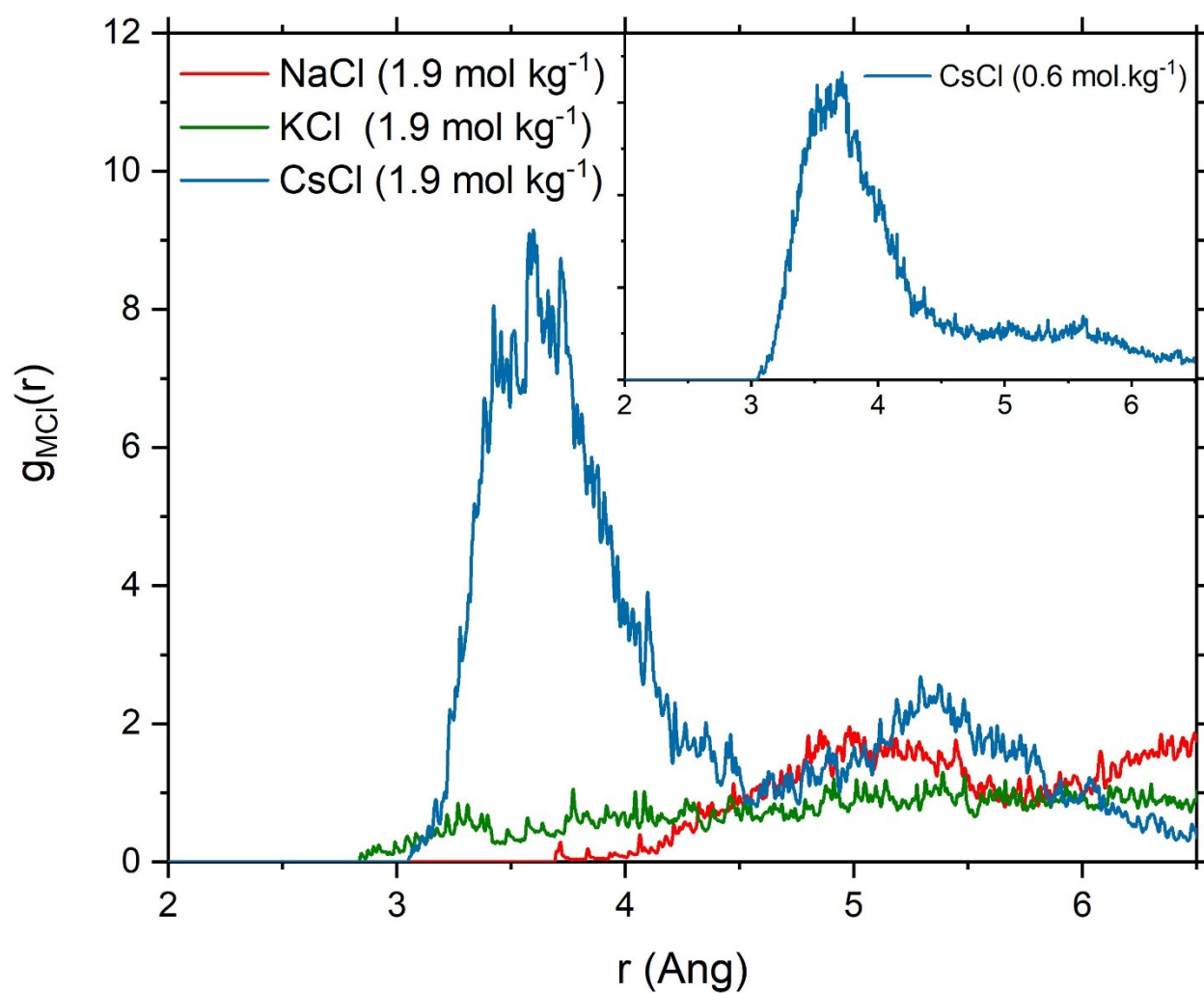


Figure S2. Metal-chloride radial distribution functions, $g_{MCl}(r)$, obtained from AIMD (PBE-D3) simulations of the aqueous electrolyte solution (1.9 mol.kg^{-1}) containing Na^+ , K^+ and Cs^+ .

Dynamics of ionic hydration shell

Water exchange around metal ions

TABLE S5. Number of accounted water exchange events ($N_{ex}^{H_2O}$) in the first coordination shells of the metal ions Li^+ , Na^+ , K^+ , Cs^+ , Mg^{2+} and Ca^{2+} , with a duration of more than $t > 5$ ps, obtained from the analysis of 50 ps of AIMD (PBE-D3) simulations of a single cation in pure water and of aqueous electrolyte solution. Values of $N_{ex}^{H_2O}$ normalized to the number of metal ions in solution. Mean residence time (MRT) of water molecules in the first hydration shell of the

$$MRT = \frac{CN_{av} \times t_{sim}}{N_{ex}^{H_2O}}$$

ion computed using the expression in mol.kg⁻¹.

. Values of MRT in ps. Concentration (b)

	b	CN	t_{sim} (ps)	$N_{ex}^{H_2O}$	$N_{ex}^{H_2O} / 10$	MRT
Li ⁺	0.9	4.0	50	17.0	3.4	11.8
LiCl	1.9	3.0	50	7.0	1.4	21.4
Na ⁺	0.9	5.1	50	233.0	46.6	1.1
NaCl	0.9	5.1	50	178.0	35.6	1.4
	1.9	5.0	50	189.5	37.9	1.3
	3.8	4.7	50	183.3	36.7	1.3
K ⁺	0.9	6.2	50	729.0	145.8	0.4
KCl	0.9	4.8	50	529.0	105.8	0.5
	1.9	5.5	50	688.0	137.6	0.4
	3.9	3.9	50	679.0	135.8	0.3
Cs ⁺	0.9	5.9	50	1357.0	271.4	0.2
CsCl	1.9	6.1	50	961.0	192.2	0.3
Mg ²⁺	0.9	6.0	50	0.0	0.0	–
MgCl ₂	1.9	6.0	50	0.0	0.0	–
MgSO ₄	1.9	4.0	50	0.0	0.0	–
Ca ²⁺	0.9	6.0	500	49	1.0	61.2
CaCl ₂	1.9	6.8	50	28.0	5.6	12.1
CaSO ₄	1.9	6.9	50	0.0	0.0	11.8
H ₂ O	–					

Free energy profiles of metal ion dehydration

The interatomic forces in *ab initio* MD are derived from the electronic structure,^{10,11} usually in the framework of density functional theory,¹² providing the capability of studying non-additivity effects in the dynamics of ions solvation shells, which is important when simulating ionic solutions.¹³ However, the computational cost of *ab initio* MD limits the size of simulated aqueous solutions (few hundreds of water molecules) and the time of the simulation (<100 ps). These restraints limit the characterization of the dynamics of solvent exchange in the first hydration shell of metal ions such as Mg²⁺, which mean residence time in the first hydration shell is of the order of microseconds.^{14,15} We have complemented the results from *ab initio* MD with classical metadynamics MD (CμMD) simulations (**Fig. S3**), which have been used to elucidate the water exchange reaction pathways around metal ions. Classical MD simulations of 1 ion (Li⁺, Na⁺, Mg²⁺ and Ca²⁺) were performed using Gromacs 2016.3.¹⁶ The leapfrog algorithm with a time step of 2 fs was used to integrate the equations of motion. Simulations were conducted in the isothermal (NVT) and isothermal-isobaric (NPT) ensembles at the target temperature T = 300 K and pressure P = 1 bar. The velocity rescale thermostat and the isotropic Parrinello-Rahman barostat were used with 0.4 ps and 2.0 ps as the thermostat and barostat relaxation times, respectively. The electrostatic forces were calculated utilizing the particle-mesh Ewald approach. A cutoff of 12 Å was used for both LJ/Coulombic interactions. Free energy calculations were conducted using the well-tempered metadynamics-biased MD method,¹⁷ using Gromacs 2016.3 equipped with the Plumed 2.4.1 plugin.¹⁸ CμMD simulations were conducted to compute the free energy profiles associated with the water exchange around the metal ion using, as the collective variable, the ion–water coordination number (CN). The reaction coordinate for rare events can be a multidimensional function of several geometric parameters. Exploring the dynamical aspects of the CN reaction coordinate allows one to examine the ability of a hydrated ion to explore the transition mechanism between under- and over-coordinated states during the dynamics of ion solvation.¹⁹ The CN was defined using the continuously differentiable function:

$$CN = \sum_i \frac{1 - \left(\frac{r_i - d_0}{r_0}\right)^n}{1 - \left(\frac{r_i - d_0}{r_0}\right)^m} \quad (1)$$

where $r_0 = 1.1$ Å, $d_0 = 1.9$ Å, $n = 4$, $m = 8$, r_i is the distance between the magnesium and the oxygen of i -th water molecule.²⁰ The free energy profiles were constructed by running classical well-tempered metadynamics-biased MD (CμMD) simulations with Gaussians laid every 1 ps and with an initial height equal to $k_B T$. The Gaussian widths were 0.2 and 0.1 along with the distance and coordination number (CN), respectively. CμMD simulations were run for a period of 1 μs to achieve convergent free energy profiles as a function of the ion–water coordination number.

Compared with literature values, for Mg²⁺ the Gibbs free energy difference between the 6- and 5-coordinated species ($\Delta G_{6 \rightarrow 5} = +29$ kJ mol⁻¹) in **Fig. S4.1** is in excellent agreement with the value obtained using *ab initio* MD ($\Delta G_{6 \rightarrow 5} = +27$ kJ mol⁻¹) using the HCTC functional;²¹ the free energy of activation ($\Delta^\ddagger G$) between these two coordination states computed using our classical metadynamics MD simulations ($\Delta^\ddagger G_{6 \rightarrow 5} = +32$ kJ mol⁻¹) is also in excellent agreement with the *ab initio* MD value ($\Delta^\ddagger G = 30$ kJ mol⁻¹) reported by Ikeda et al.²¹ For Ca²⁺, $\Delta G_{7 \rightarrow 6} = 5$ kJ mol⁻¹ was obtained from our classical metadynamics and $\Delta G_{7 \rightarrow 6} = -8$ kJ mol⁻¹ from *ab initio* MD (HCTC functional);²¹ classical MD predict the 7-coordinated species to be the most stable and *ab initio* MD predict the 6-coordinated species to be the most stable. Excellent agreement is achieved for the free energy of activation: $\Delta^\ddagger G_{7 \rightarrow 6} = 11$ kJ/mol from our classical MD and $\Delta^\ddagger G_{6 \rightarrow 7} = 10$ kJ mol⁻¹ from *ab initio* MD. For Na⁺, our simulations show that the free energy difference ($\Delta G = 0.5$ kJ mol⁻¹) and activation barrier ($\Delta^\ddagger G = 2.5$ kJ mol⁻¹) of the 5- and 6-

coordinates species is very low; *ab initio* MD free energy calculations by Galib et al. (revPBE-D3) show similar profiles, with an easy interconversion between the 5 and 6 coordinated spaces (activation energy < 4 kJ mol⁻¹).³

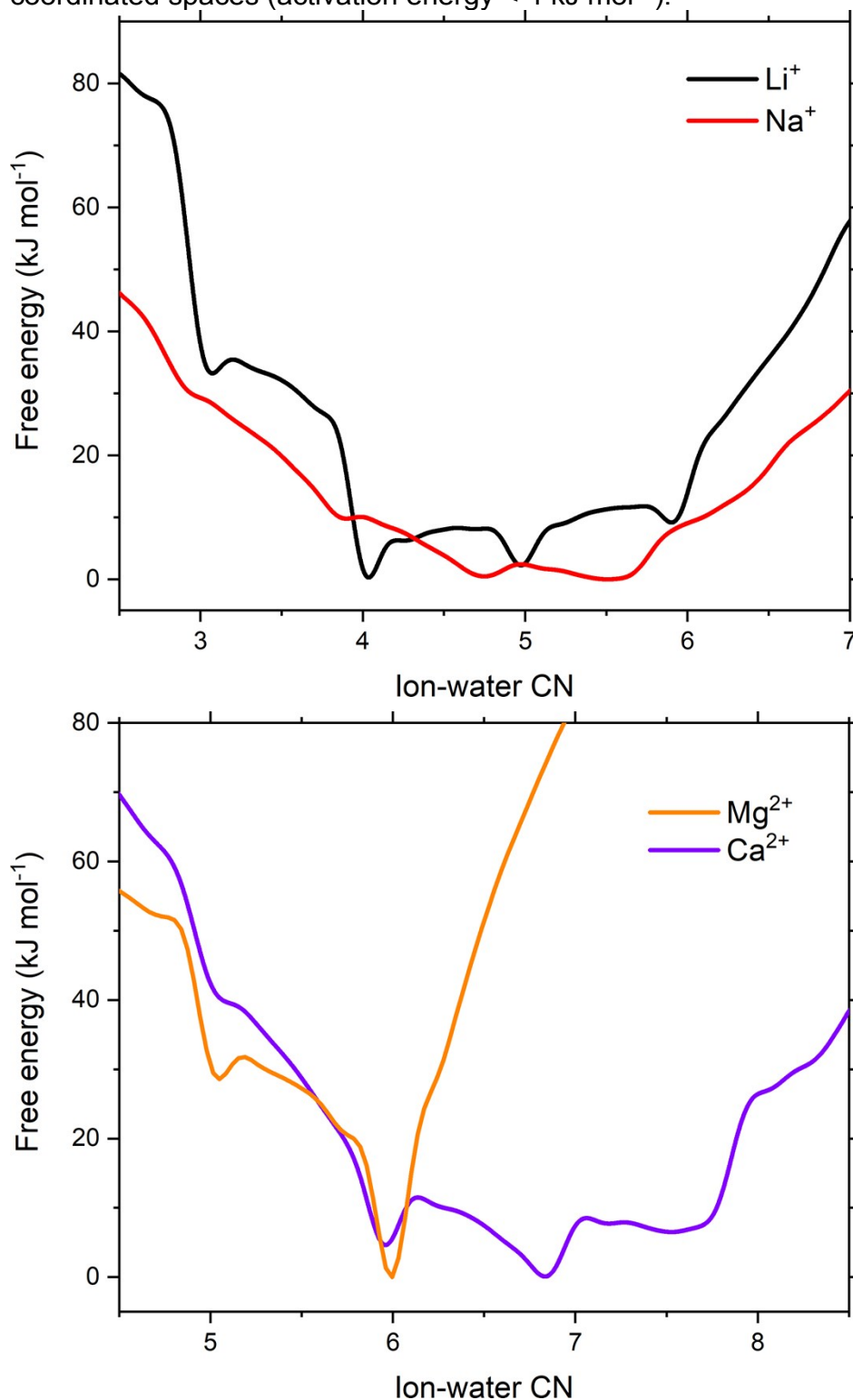


FIGURE S3. Free energy as a function of the ion–water coordination number computed from well-tempered metadynamics-biased MD (CM μ D) method. Minima deviate slightly from the expected integer coordination values due to numerical factors arising from the need

to define a smooth and continuous analytic definition of the coordination number for use as a collective variable (see **Eq 1**).

Velocity autocorrelation function of the metal ions

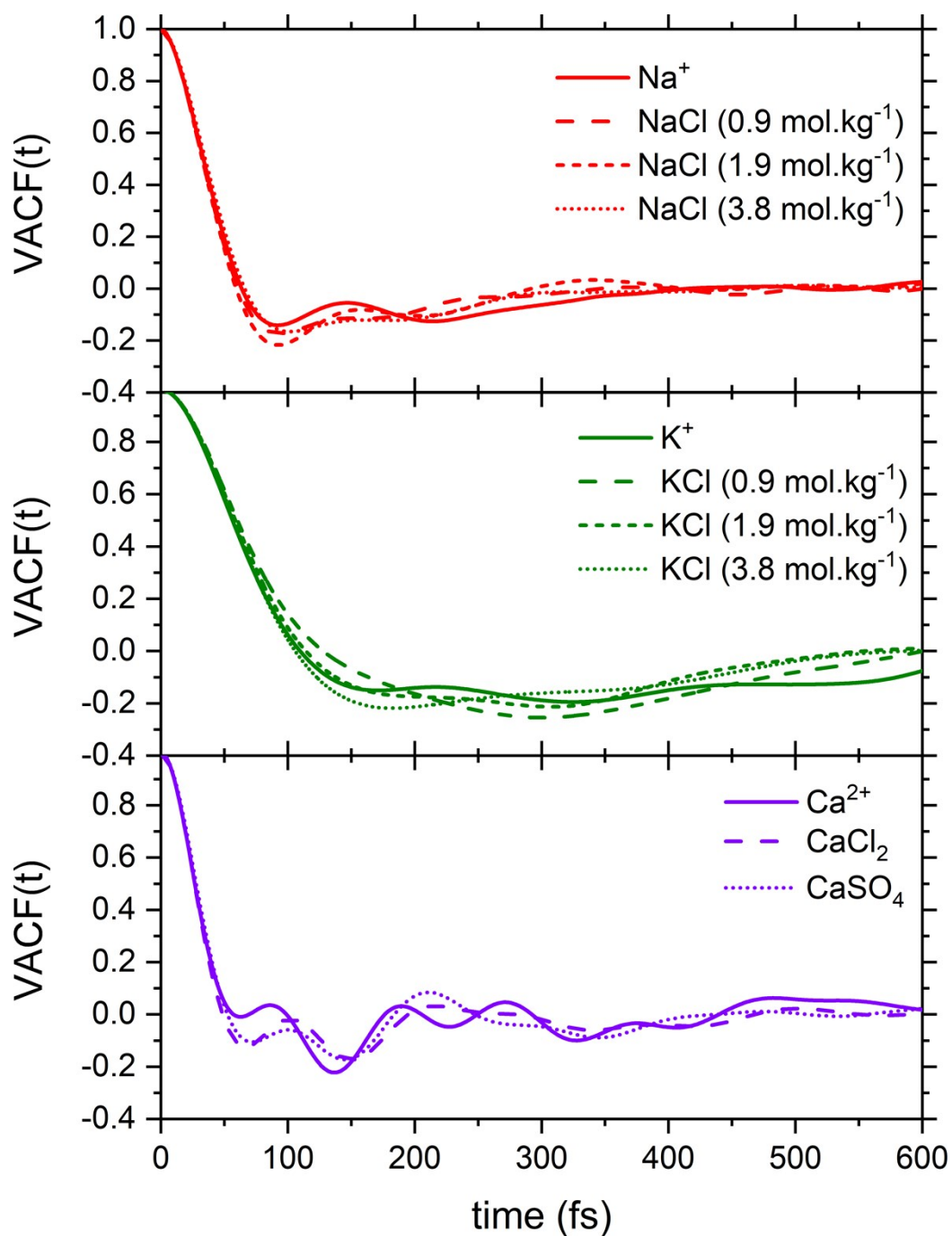


FIGURE S4. Velocity autocorrelation functions (VACF) of Na^+ , K^+ and Ca^{2+} obtained from AIMD (PBE-D3) simulations of the hydrated cation (single ion, no counterions) and of aqueous electrolyte solutions.

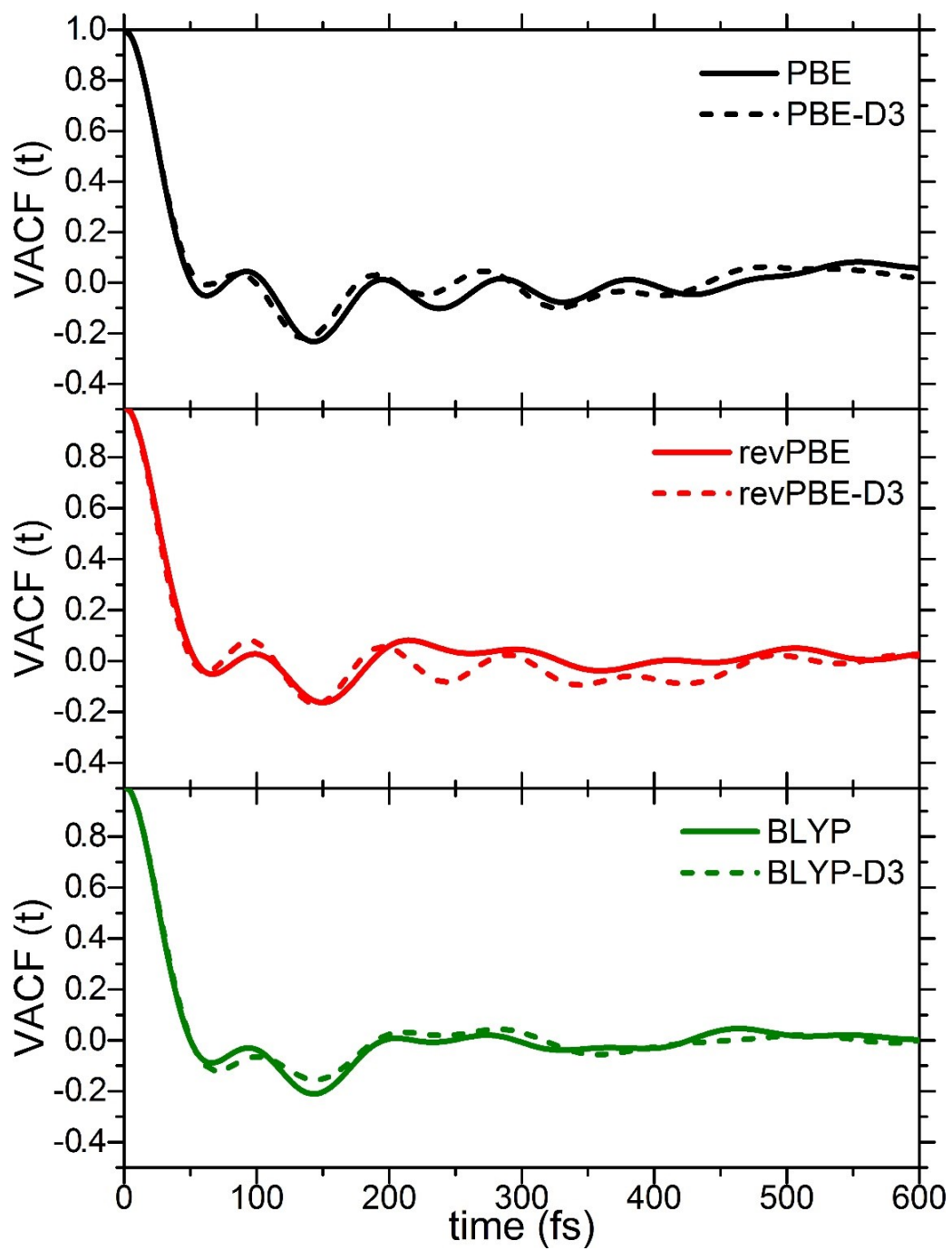


FIGURE S5. Velocity autocorrelation functions (VACF) of Ca^{2+} obtained from AIMD simulations of the hydrated calcium ion (single Ca^{2+} , no counterions) using different DFT methods.

Hydrogen bond statistics

TABLE S6. The distribution of the number of hydrogen-bonds (HBs) per water molecule in pure liquid water, in aqueous solutions containing a single hydrated ion (no counterions), and of aqueous electrolyte solution at different concentrations. The values given are percentages of molecules with the given number of hydrogen bonds. Values obtained from the analysis of AIMD (PBE-D3) simulations. Concentration (b) in mol.kg⁻¹.

System	b	Number of HBs (%)						average
		f_0	f_1	f_2	f_3	f_4	f_5	
Li ⁺	0.9	0.0	0.7	5.0	18.5	71.1	4.6	3.74
LiCl	1.9	0.1	1.7	7.6	27.5	61.6	1.5	3.53
Na ⁺	0.9	0.0	0.5	4.9	21.4	68.4	4.7	3.72
NaCl	0.9	0.1	1.2	8.3	27.9	58.8	3.7	3.55
	1.9	0.1	1.6	10.2	36.9	48.3	2.8	3.40
	3.8	0.5	6.4	20.2	38.2	32.1	2.5	3.03
K ⁺	0.9	0.0	0.3	3.0	16.3	75.9	4.5	3.81
KCl	0.9	0.1	1.0	7.0	25.6	62.5	3.8	3.61
	1.9	0.1	1.8	12.3	35.6	47.1	3.0	3.37
	3.9	0.7	4.8	18.6	30.1	43.5	2.4	3.18
Cs ⁺	0.9	0.0	0.2	3.0	17.6	74.3	4.9	3.81
CsCl	1.9	0.3	1.6	8.5	28.8	58.6	2.2	3.50
Mg ²⁺	0.9	0.1	1.5	8.2	18.7	63.1	8.4	3.69
MgCl ₂	1.9	0.1	5.0	25.6	35.5	32.5	1.3	2.99
MgSO ₄	1.9	0.9	6.1	13.1	27.4	50.9	1.6	3.26
Ca ²⁺	0.9	0.0	0.9	7.6	19.3	64.4	7.9	3.71
CaCl ₂	1.9	0.4	7.8	22.6	32.0	35.3	1.8	3.00
CaSO ₄	1.9	0.9	7.2	16.9	36.5	36.7	1.7	3.06
H ₂ O	–	0.0	0.3	4.6	19.8	70.7	4.6	3.75

Calculation of time correlation functions

Protocol

The methodology below has been adopted to compute the reorientation time correlation functions (TCF), $P_1(t)$, defined as the first-order Legendre polynomials of water dipole, a unit bisector of the H–O–H angle ($\vec{\mu}$).

1. Calculate dipole vectors of each water molecule at all time step from trajectory, $\mu_i(t)$: dipole vectors of i^{th} water molecule at time t .
2. Compute the inner product between the unit vectors defining the orientation of the dipole moment of the i -th water molecule at the time origin t_o and time t : $u_i(t_o) \cdot u_i(t)$.
3. The first-order Legendre polynomial TCF is obtained from the average over whole water molecule in the simulation box (or in the subpopulation of water molecule):

$$P_1^o(t) = \frac{1}{N_w} \sum_i^{N_w} u_i(t_o) \cdot u_i(t) \quad (\text{S1})$$

4. The first-order Legendre polynomial TCF is obtained for several time origin and overlapping intervals $[0, t]$ of equal time length (Figure S3).
5. The value of $P_1(t)$ in the time intervals $[0, t]$ is obtained from the average of $P_1^o(t)$:

$$P_1(t) = \frac{1}{N_o} \sum_i^{N_o} P_1^o(t) \quad (\text{S2})$$

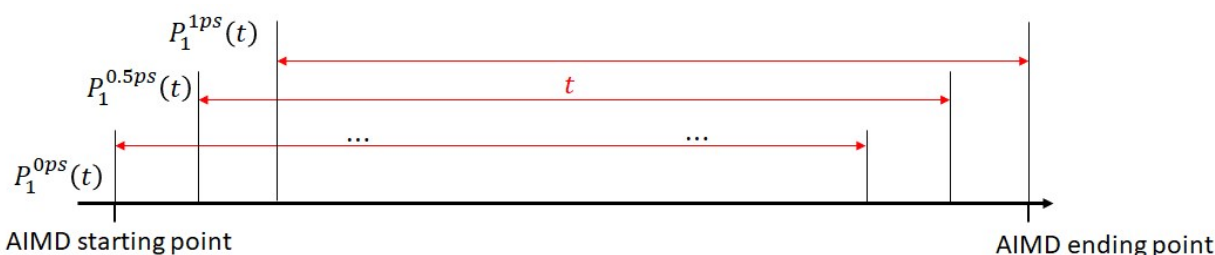


FIGURE S6. Procedure adopted to calculate the value of $P_1^o(t)$ for several time origins and overlapping time of equal time length, $[0, t] = 16000$ fs.

Time average of time correlation functions over several time origin

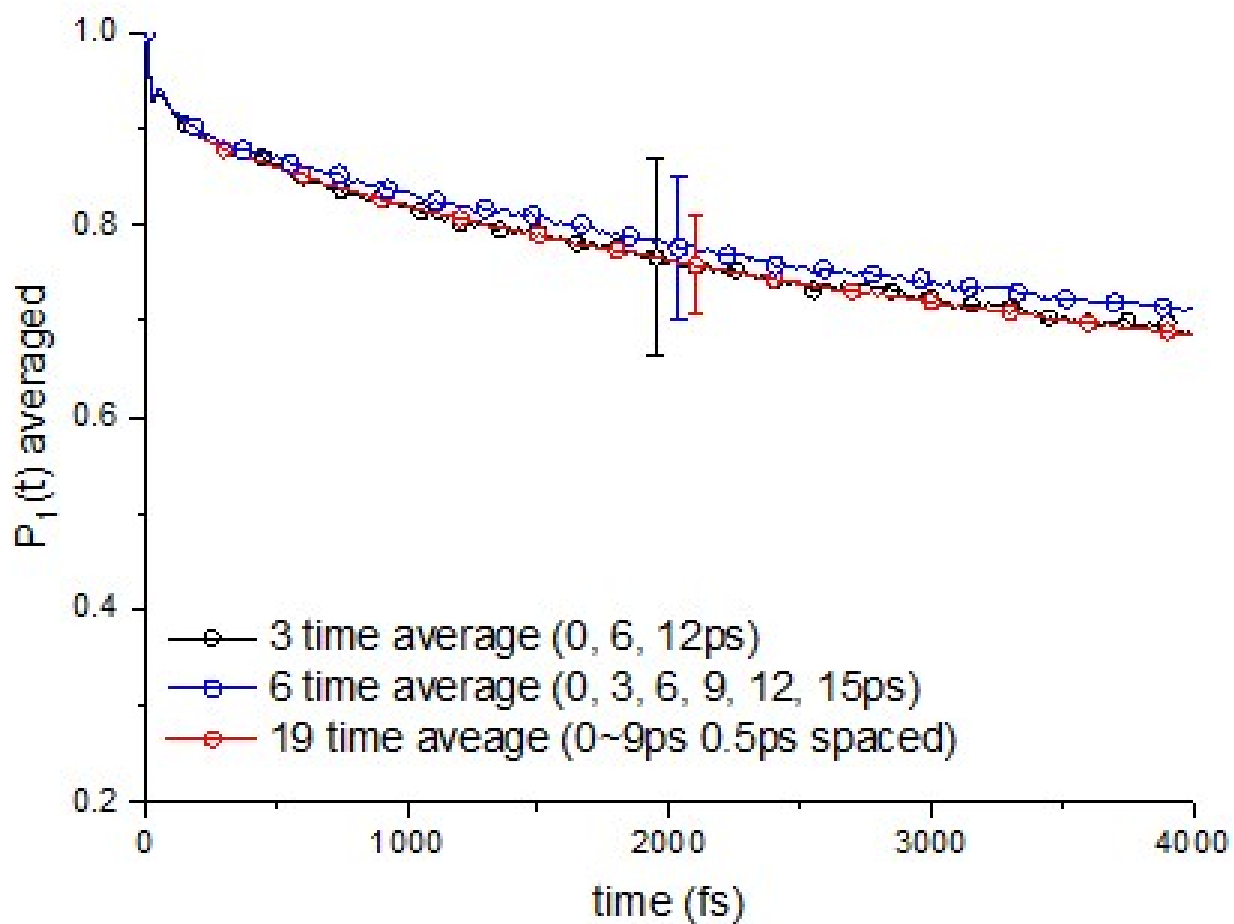


FIGURE S7. First-order Legendre reorientational TCFs, $P_1(t)$, of water in solutions of $MgCl_2$ obtained using indicated time origins. Standard deviation (error bars) decreases by increasing the number of time origins.

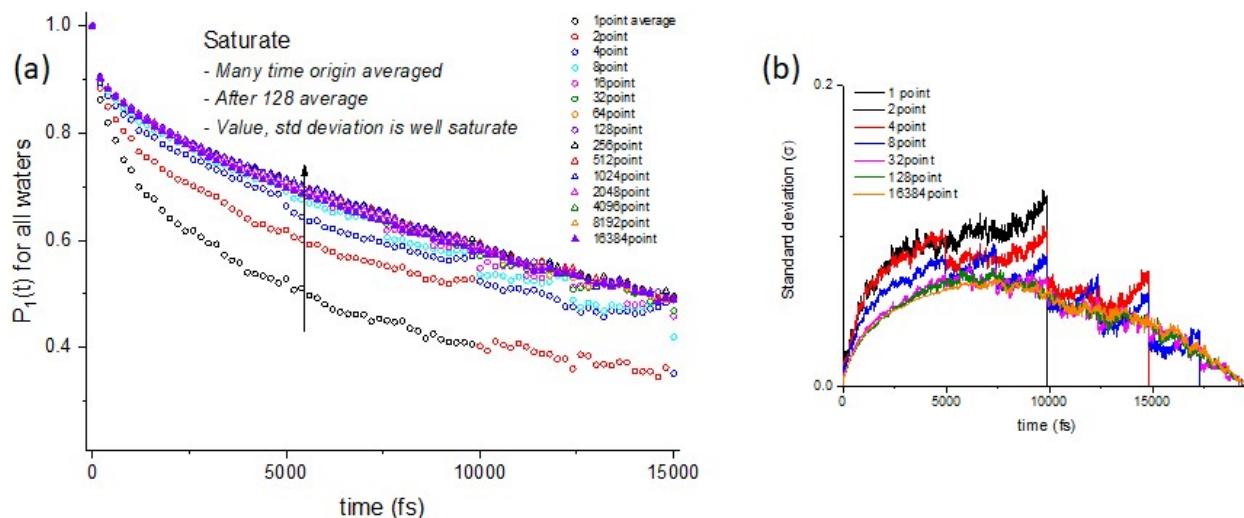


FIGURE S8. First-order Legendre reorientational TCFs, $P_1(t)$, of water in solutions of $MgCl_2$ obtained using indicated time origins. Behavior of the reorientation decay (a) and of the standard deviation (b) with the number of time origins used in the evaluation of $P_1(t)$ (Eq. S2). Time interval used to compute $P_1(t)$ is 16000 steps. Dipole correlation and standard deviation reach convergence after 128 origin time averages.

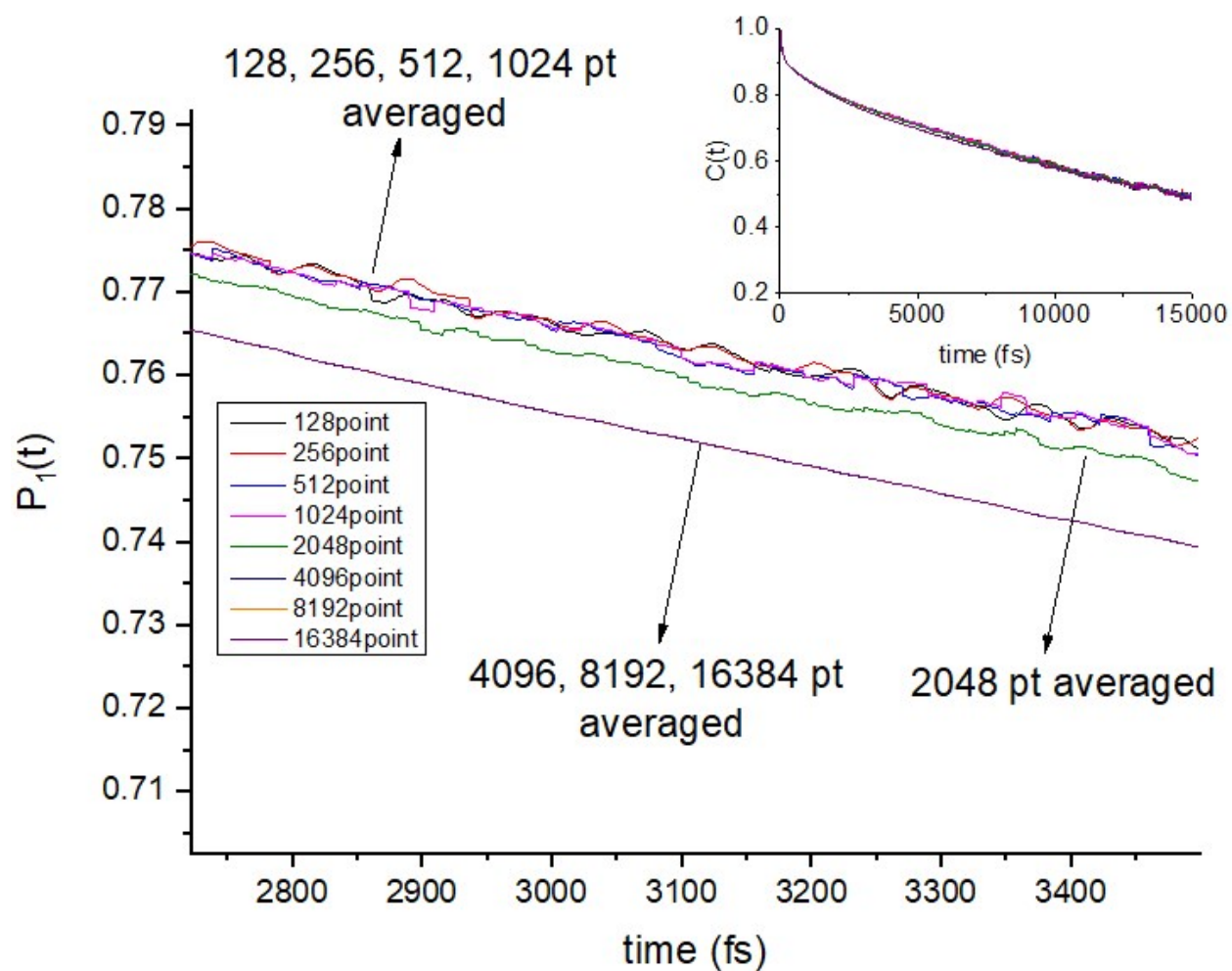


FIGURE S9. First-order Legendre reorientational TCFs, $P_1(t)$, of water in solutions of MgCl_2 obtained using indicated time origins. The plots in the time interval [2.8–3.4 ps] show that differences in the computed values of $P_1(t)$ are less than 0.01 (2%).

References

- 1 A. P. Lyubartsev, K. Laasonen and A. Laaksonen, Hydration of Li⁺ ion. An ab initio molecular dynamics simulation, *J. Chem. Phys.*, 2001, **114**, 3120–3126.
- 2 T. T. Duignan, G. K. Schenter, J. L. Fulton, T. Huthwelker, M. Balasubramanian, M. Galib, M. D. Baer, J. Wilhelm, J. Hutter, M. Del Ben, X. S. Zhao and C. J. Mundy, Quantifying the hydration structure of sodium and potassium ions: taking additional steps on Jacob's Ladder, *Phys. Chem. Chem. Phys.*, 2020, 10641–10652.
- 3 M. Galib, M. D. Baer, L. B. Skinner, C. J. Mundy, T. Huthwelker, G. K. Schenter, C. J. Benmore, N. Govind and J. L. Fulton, Revisiting the hydration structure of aqueous Na⁺, *J. Chem. Phys.*, 2017, **146**, 84504.
- 4 V. A. Glezakou, Y. Chen, J. L. Fulton, G. K. Schenter and L. X. Dang, Electronic structure, statistical mechanical simulations, and EXAFS spectroscopy of aqueous potassium, *Theor. Chem. Acc.*, 2006, **115**, 86–99.
- 5 S. Roy and V. S. Bryantsev, Finding Order in the Disordered Hydration Shell of Rapidly Exchanging Water Molecules around the Heaviest Alkali Cs⁺ and Fr⁺, *J. Phys. Chem. B*, 2018, **122**, 12067–12076.
- 6 D. Di Tommaso and N. H. de Leeuw, First Principles Simulations of the Structural and Dynamical Properties of Hydrated Metal Ions Me²⁺ and Solvated Metal Carbonates (Me = Ca, Mg, and Sr), *Cryst. Growth Des.*, 2010, **10**, 4292–4302.
- 7 K. M. Callahan, N. N. Casillas-Ituarte, M. Roeselová, H. C. Allen and D. J. Tobias, Solvation of magnesium dication: molecular dynamics simulation and vibrational spectroscopic study of magnesium chloride in aqueous solutions., *J. Phys. Chem. A*, 2010, **114**, 5141–5148.
- 8 I. Bakó, J. Hutter and G. Pálinkás, Car–Parrinello molecular dynamics simulation of the hydrated calcium ion, *J. Chem. Phys.*, 2002, **117**, 9838–9843.
- 9 J. L. Fulton, S. M. Heald, Y. S. Badyal and J. M. Simonson, Understanding the effects of concentration on the solvation structure of Ca²⁺ in aqueous solution. I: The perspective on local structure from EXAFS and XANES, *J. Phys. Chem. A*, 2003, **107**, 4688–4696.
- 10 R. Car and M. Parrinello, Unified Approach for Molecular Dynamics and Density-Functional Theory, *Phys. Rev. Lett.*, 1985, **55**, 2471–2474.
- 11 D. Marx and J. Hutter, *Ab initio molecular dynamics: Theory and implementation*, John von Neumann Institute for Computing, Julich, 2000, vol. 1.
- 12 W. Kohn and L. J. Sham, Self-Consistent Equations Including Exchange and Correlation Effects, *Phys. Rev.*, 1965, **140**, A1133–A1138.
- 13 Y. Ding, A. Hassanali and M. Parrinello, Anomalous water diffusion in salt solutions., *Proc. Natl. Acad. Sci. U. S. A.*, 2014, **111**, 3310–5.
- 14 A. Bleuzen, L. Helm and A. E. Merbach, Water exchange on magnesium(II) in aqueous solution: A variable temperature and pressure ¹⁷O NMR study, *Magn. Reson. Chem.*, 1997, **35**, 765–773.

- 15 X. Zhang, P. Alvarez-Lloret, G. Chass and D. Di Tommaso, Interatomic potentials of Mg ions in aqueous solutions: structure and dehydration kinetics, *Eur. J. Mineral.*, 2019, **31**, 275–287.
- 16 D. Van Der Spoel, E. Lindahl, B. Hess, G. Groenhof, A. E. Mark and H. J. C. Berendsen, GROMACS: Fast, flexible, and free, *J. Comput. Chem.*, 2005, **26**, 1701–1718.
- 17 A. Barducci, G. Bussi and M. Parrinello, Well-Tempered Metadynamics: A Smoothly Converging and Tunable Free-Energy Method, *Phys. Rev. Lett.*, 2008, **100**, 20603.
- 18 G. A. Tribello, M. Bonomi, D. Branduardi, C. Camilloni and G. Bussi, PLUMED 2: New feathers for an old bird, *Comput. Phys. Commun.*, 2014, **185**, 604–613.
- 19 S. Roy, M. D. Baer, C. J. Mundy and G. K. Schenter, Reaction Rate Theory in Coordination Number Space: An Application to Ion Solvation, *J. Phys. Chem. C*, 2016, **120**, 7597–7605.
- 20 P. Raiteri, J. D. Gale, D. Quigley and P. M. Rodger, Derivation of an Accurate Force-Field for Simulating the Growth of Calcium Carbonate from Aqueous Solution: A New Model for the Calcite Water Interface, *J. Phys. Chem. C*, 2010, **114**, 5997–6010.
- 21 T. Ikeda, M. Boero and K. Terakura, Hydration properties of magnesium and calcium ions from constrained first principles molecular dynamics, *J. Chem. Phys.*, , DOI:10.1063/1.2768063.